PROPERTIES OBTAINED BY CHROMIUM-CONTAINING MATERIAL

Sigurd Berg, Barbara Maroli
Höganäs AB
Sweden

ABSTRACT

Chromium as an alloying element in PM steel is of great interest due to its low cost, positive effect on hardenability and recycling advantages in the scrap phase of PM parts.

The conversion from conventional steels to PM steels for large-scale production of components is primarily based on cost advantages. Traditionally, however, the cost for alloying elements in PM steels is higher than that of wrought steel. By utilization of a low cost alloying element such as chromium in PM, competitiveness can be improved.

This paper compares a new prealloyed powder containing chromium and molybdenum with conventional powders. Static and dynamic properties are evaluated after sintering at 2050°F and 2280° F (1120°C and 1250°C). Mechanical performance after cooling in the range 1.8 to 9°F/s will also be shown.

INTRODUCTION

Powder metallurgy is a strong growing market. Since most of the parts made by P/M are for the automotive industry, cost is a major driving force. In recent years new processing techniques and alloying systems have been developed in order to increase the performance/cost ratio. Pre-alloyed materials have become more and more used in the PM industry. One reason for this is that the core of the iron particle is strengthened and as a consequence the mechanical properties are enhanced. Molybdenum is the main pre-alloying element used in the PM industry. Reasons are the relative small impact molybdenum has on the compressibility compared to other alloying elements and the good response in hardenability. Chromium as a pre-alloying element has an even higher performance/cost ratio compared to molybdenum and is therefore of great interest for the future. Chromium is of interest due to low cost, even distribution if pre-alloyed and greater possibility to recycle then copper containing materials. A consequence of pre-alloying compared to mixing is the reduction of scatter in dimensional change.

In this paper a water atomized pre-alloyed powder with 1.5% Chromium and 0.2% Molybdenum designated Astaloy CrL was evaluated. The material was compared to the diffusion alloyed powder D. AB and the Fe-Cu-C system in respect of static and dynamic properties achieved after conventional sintering as well as high temperature sintering. For sinterhardening, Astaloy CrL is compared to the diffusion alloyed powder D. DH-1.

EXPERIMENTAL

Chemical composition of the investigated materials are shown in table 1.

Table 1. Composition for the Materials used.

Material		Chromium (%)	Molybdenum (%)	Copper (%)	Nickel (%)
A	Astaloy CrL	1.5**	0.2**		
B	FC-0200/0208			2	
C	D. AB (FD-0205/0208)		0.5*	1.5*	1.75*
D	D. DH-1		1.5**		2*

* Diffusion bonded alloying element. ** Pre-alloyed alloying element.

In table 2 the admixed graphite amount for respectively material is shown.

Table 2. Admixed Mixed Graphite.

Material		Graphite (%)
A	Astaloy CrL	0.2 - 0.8
B	FC-0200/0208	0.2 - 0.8
C	D. AB (FD-0205/0208)	0.3 - 0.8
D	D. DH-1	0.6/0.8

Compressibility and mechanical properties are evaluated according to ISO 3927 and ISO 2740-1986 respectively. For cold compaction, 0.8% Amide wax is used. For warm compaction, DENSMIX™ powder compacted at a die temperature of 302°F (150°C) and powder temperature of 266°F (130°C) was used. The lubricant amount is 0.6%. Sintering at 2050°F (1120°C) was performed in a laboratory belt furnace for 30 minutes in 90/10 N_2/H_2. The cooling rate was 1.4°F/s (0.8°C/s) except for the sinterhardening evaluation where the cooling rate is 9°F/s (5°C/s). Hydrocarbon (methane) was used for carbon control. An oxygen probe was used for the partial pressure of oxygen measurement. Sintering at 2280°F (1250°C) was performed in a laboratory batch furnace with 90/10 N_2/H_2 without methane additions. The cooling rate was 1.8°F/s (1°C/s).

RESULTS AND DISCUSSION

Compressibility

The type and amount of an alloying element affects the compressibility. In the pre-alloyed state solution hardening causes reduced compressibility. The relationship regarding compressibility for the materials were evaluated at three compacting pressures with die wall lubrication, table 3. Here it is seen that material B has the highest compressibility. Diffusion bonding of nickel, copper and molybdenum on plain iron, material C follows with a density of 7.16g/cm^3. Diffusion bonded copper on a pre-alloyed powder with 1.5% molybdenum, material D has a compressibility of 7.08g/cm^3. Material A, pre-alloyed 1.5% chromium and 0.2% molybdenum, has a compressibility

of 7.04g/cm^3 tsi. The difference in compressibility between the materials decreases at higher compacting pressures.

Table 3. Compressibility. Die Wall Lubrication.

Material	29 tsi (400 Mpa)	43.5 tsi (600 Mpa)	58 tsi (800 Mpa)
A. Astaloy CrL	6.55	7.04	7.32
B. FC-0200/0208	6.77	7.19	7.45
C. D. AB (FD-0205/0208)	6.73	7.16	7.44
D. D. DH-1	6.62	7.08	7.36

Material performance for Astaloy CrL, material A.

Density plays an important role in the manufacturing of PM parts. The strong relationship between sintered density and mechanical properties is well known in the PM industry. For material A, the effect of increased compacting pressure on sintered density is shown in table 4. Admixed graphite for evaluation of mechanical properties is 0.45 and 0.85%. At the lower graphite addition sintered density increases from 6.52 to 7.14 g/cm^3 as the compacting pressure is increased from 29 to 58 tsi. Dimensional change is almost independent of compacting pressure. Increased carbon content decreases the shrinkage from 0.12 to 0.04%. Mechanical properties like UTS and yield strength increases with increased compaction pressure. An increase in UTS from 79.3 to 114.7 ksi is achieved for the higher carbon content. Yield strength follows the same trend. Hardness increases with carbon content reaching HRC values of 25 (269 HV10) at the highest carbon content and compacting pressure. Gain in elongation at increased compacting pressure is also obtained.

Table 4. Mechanical Properties of Material A; Astaloy CrL with 0.43% and 0.83% C.

Graphite %	Compacting pressure tsi (MPa)	SD g/cm^3	DC* %	UTS ksi (MPa)	YS ksi (MPa)	HV10	Elong %	Carbon %
0.45	29 (400)	6.52	-0.13	68.3 (471)	53.9 (372)	129	1.1	
	43.5 (600)	6.92	-0.12	85.7 (591)	67.4 (465)	173	1.7	0.43
	58 (800)	7.14	-0.12	93.5 (645)	73.1 (504)	193	1.9	
0.85	29 (400)	6.51	-0.04	79.3 (547)	78.6 (542)	206	0.2	
	43.5 (600)	6.90	-0.03	107.6 (742)	96.9 (668)	245	0.5	0.83
	58 (800)	7.07	-0.04	114.7 (791)	106.0 (731)	267	0.4	

* die to sintered.

Warm compaction has been adopted in the PM industry in order to increase density. Other benefits from the warm compaction technique are;

- Even density distribution -> tighter tolerances,
  -> higher strength, especially fatigue
- Increased green strength -> possibility to green machining,
  -> easier handling of green parts
- Possibility to meet density demand at lower compacting pressure -> smaller presses can be used [ref. 1].

At a compacting pressure of 43.5 tsi (600MPa) the density increases with 0.2g/cm^3 if warm compaction is used as shown in table 5. At a compacting pressure of 58 tsi (800Mpa) the gain is ~0.15g/cm^3.

Table 5. Sintered Density after Cold and Warm Compaction of Material A, Astaloy CrL, 0,45% added graphite.

Comp. Press tsi (Mpa)	Cold compaction g/cm^3	Warm compaction g/cm^3
43.5 (600)	6.92	7.12
58.0 (800)	7.14	7.28

Utilising warm compaction makes it possible to reduce the required compacting pressure by 14 tsi in order to reach the same sintered density.

If warm compaction is used mechanical properties are increased due to the increase in sintered density, see table 6. UTS of 93 to 101 ksi is reached for the lower carbon content. The corresponding yield strength is in the range from 70 to 76 ksi with an elongation of 2.5 to 2.9%. At a carbon content of 0.76% the UTS is in the range from 108 to 120 ksi with an elongation of 1%. Compared to cold compaction the elongation is higher at the same sintered density. This is related to the decreased pore size obtained by warm compaction [2]

Table 6. Mechanical Properties Obtained by Warm Compaction of Material A. Astaloy CrL.

Graphite %	Compacting pressure Tsi (Mpa)	SD g/cm^3	DC* %	UTS ksi (Mpa)	YS ksi (Mpa)	HV10	Elong %	Carbon %
0.45	43.5 (600)	7.12	-0.03	93.2 (643)	70.0 (486)	196	2.5	
	50.7 (700)	7.22	-0.04	96.4 (665)	72.5 (500)	200	2.5	0.38
	58 (800)	7.28	-0.05	101.4 (699)	76.1 (525)	214	2.9	
0.85	43.5 (600)	7.07	-0.03	132.1 (911)	108.2 (746)	262	1.1	
	50.7 (700)	7.16	-0.03	139.1 (959)	115.2 (794)	270	1.2	0.76
	58 (800)	7.22	-0.03	143.1 (987)	120.4 (830)	275	1.0	

* die to sintered.

The response in mechanical properties, cold compared to warm compaction for material A within the carbon range of 0.2 to 0.8% is show in figure 1.

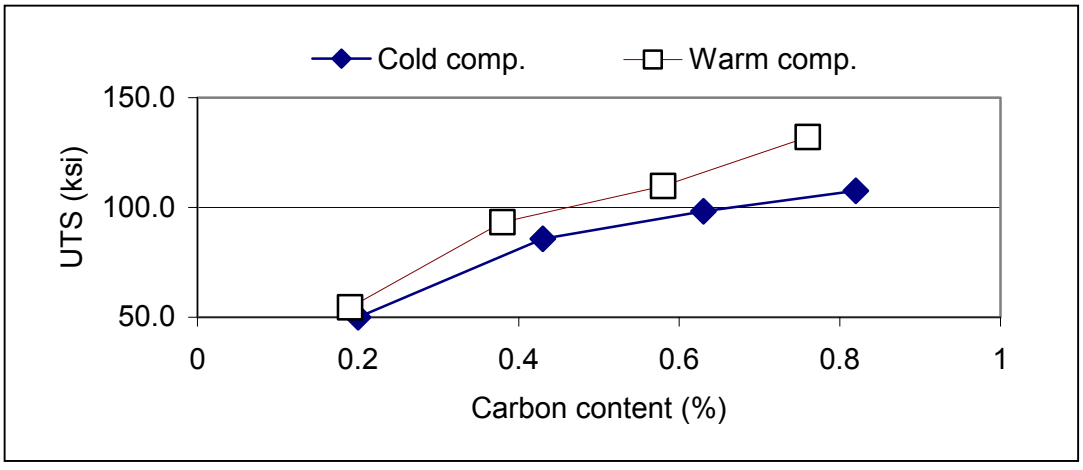
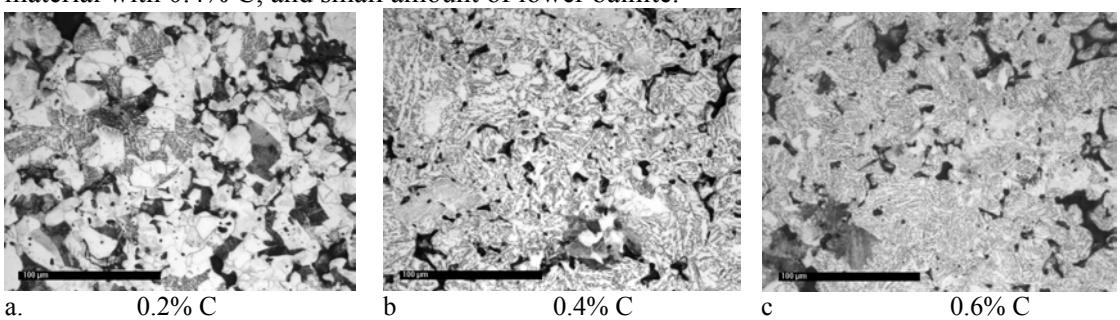


Figure 1. UTS vs carbon content for material A, Astaloy CrL compacted at 43.5 tsi and sintered at 2050°F.

The increase in mechanical properties between 0.2 and 0.4% C is due to a transformation from ferrite/perlite to bainite microstructure. At 0.8% C the mechanical properties are further increased

due to formation of lower bainite. In figure 2 a-c the microstructures at 0.2, 0.4 and 0.6% C are shown. Analysed phase amounts are 60% perlite, 20% ferrite and 20% bainite at 0.2% combined carbon content. At 0.4%C the microstructure consist of 95% bainite. 2.5% ferrite and 2.5% perlite. At 0.6% carbon the microstructure consists of upper bainite with finer carbides if compared to the material with 0.4% C, and small amount of lower bainite.



a. 0.2% C b 0.4% C c 0.6% C

Figure 2. Microstructure of material A. Astaloy CrL at different carbon content.

High temperature sintering is beneficial for chromium containing materials. The effect of increased sintering temperature on mechanical properties is shown in table 7. At 2280°F (1250°C) the shrinkage is 0.68% giving a sintered density of 7.10g/cm^3 at a compacting pressure of 43.5 tsi. A UTS of 132.4 ksi is obtained at 0.51% C. At an increased combined carbon content of 0.66% the UTS increases up to 157.6 ksi. Corresponding yield strength is 96.3 at 0.51% C and 124.7 ksi at 0.66% C. At these conditions the material has taken hardening, especially at the higher carbon content. This can be seen by the elongation which is 0.6% and hardness value of 380 HV10.

Table 6. Mechanical Properties Material A with 0.51% and 0.66% C.

Graphite %	Compacting pressure tsi (MPa)	SD g/cm^3	DC* %	UTS ksi (MPa)	YS ksi (MPa)	HV10	Elong %	Carbon %
0.65	43.5 (600)	7.10	-0.68	132.4 (913)	96.3 (664)	274	1.8	0.51
0.80	4.35 (600)	7.11	-0.69	157.6 (1087)	124.7 (860)	380	0.6	0.66

Material performance for material A compared to material B and C.

Evaluation of mechanical properties for material A-C at a fixed compacting pressure of 43.5tsi (600MPa), sintered at 2050°F (1120°C) for 30 minutes is shown in figure 3. At 0.2% combined carbon material A and B have the same tensile strength. The microstructure for both materials consists of ferrite and pearlite. Increased carbon (0.4%) change the microstructure for material A to bainite. A further increase in carbon content to 0.6% creates a mix of upper and lower bainite. At 0.8% C lower bainite is formed. For material B, increased carbon content increases the amount of perlite at the expense of the ferrite. The microstructure of material C consists mainly of perlite plus some martensite, austenite and ferrite. With increased carbon content the amount of martensite and retained austenite increases at the expense of the ferrite and perlite. The increase in properties is lower for material C compared to material A which is explained by a smaller degree of change in microstructure. At a carbon content of 0.8%, the strength level for material C is close to that of material B.

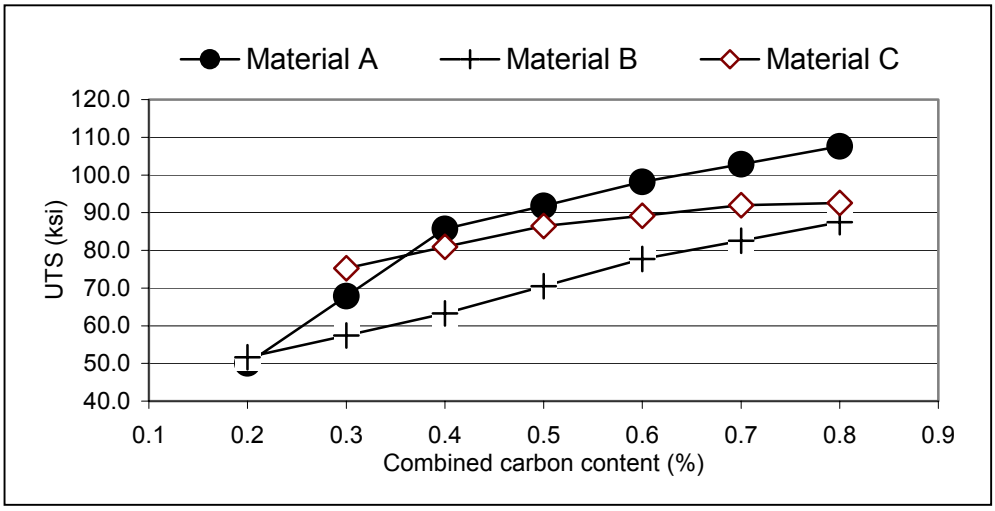


Figure 3. UTS of Astaloy CrL (A), Fe-2%Cu (B) and D.AB (C) at different carbon levels, compacting pressure 43.5tsi and sintering temperature 2050°F.

In figure 4a material A is compared to material B regarding yield strength. The trend between materials is maintained from figure 3. In figure 4b the hardness for material A excides that for material B when the combined carbon content is higher than 0.2%. This is due to the high hardenability of chromium containing materials. By increased hardness the elongation decreases as shown in figure 4c.

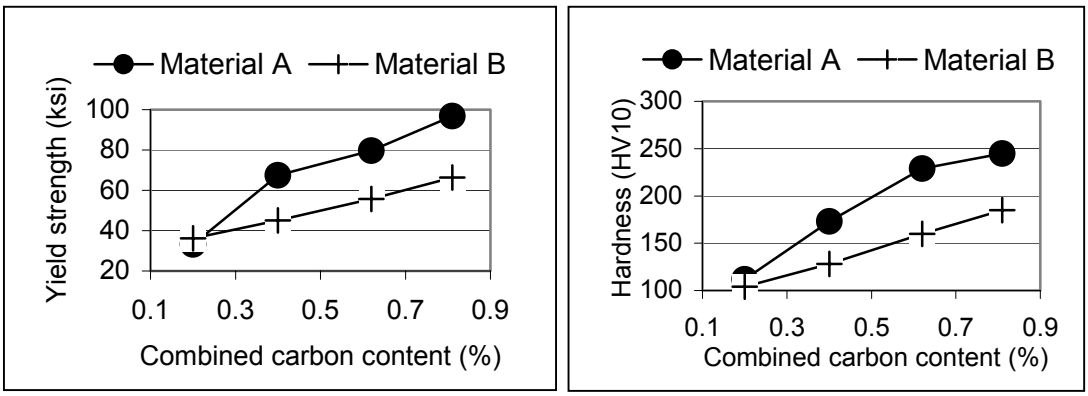


Figure 4a and b yield strength and hardness for material A (Astaloy CrL) and material B (Fe+2% Cu) at different combined carbon levels compacted at 43.5tsi (600MPa) sintered at 2050°F (1120°C).

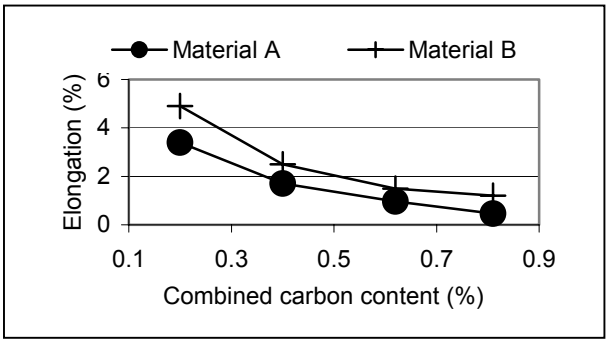
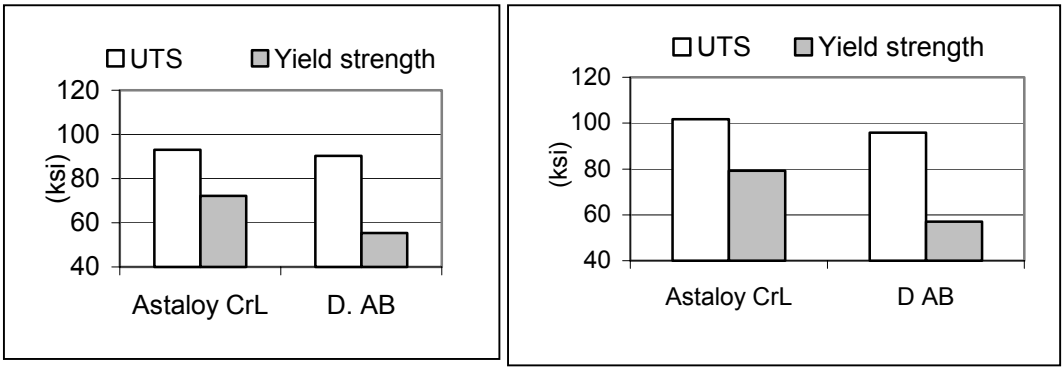


Figure 4c Elongation for material A (Astaloy CrL) and material B (Fe-2% Cu) at different combined carbon levels compacted at 43.5tsi (600MPa) sintered at 2050°F (1120°C).

The performance of material A compared to material B is higher at all investigated carbon contents except for elongation. From figure 4b and 4c at an equal hardness the elongation is the same for the both investigated materials. Obtained properties are explained by the microstructure. Material B has a ferrite pearlite microstructure throughout the investigated carbon range while material A has a transformation to bainite in the carbon range of 0.2 to 0.4%.

Mechanical properties obtained for material A at combined carbon contents above 0.4% excide the one for material C, figure 3. A closer investigation at a fixed compacting pressure of 43.5tsi (600 MPa) is shown in figure 5a. The sintered density is 6.95 g/cm^3 for material A and 7.05 g/cm^3 for material C. Combined carbon is 0.55%. UTS is slightly higher for material A while the yield strength is significantly higher, 16.7ksi (115MPa). An elongation of 1.4% is obtained for material A and 1.9% for material C

Evaluation of properties at a same sintered density of 7.1g/cm^3, figure 5b, shows an increase in difference between the two materials. Difference in yield strength is 22.2ksi (41Mpa). An elongation of 1.6% is obtained for material A and 2.2% for material C. The hardness is slightly (10 HV10) higher for material A, both at the same compacting pressure and same sintered density.



a. Fixed compacting pressure b. Fixed sintered density of 7.1g/cm^3.

Figure 5. UTS and yield strength for material A. Astaloy CrL and material C. D.AB at fixed compacting pressure of 43.5tsi (a) and fixed sintered density of 7.1g/cm^3 (b)

Dimensional change – tolerance.

Control of the dimensional change is important in order to manufacture PM parts to tight tolerances. Tolerances are affected by density and chemical difference within the compacted part before sintering. In order to compare the performance of material A Astaloy CrL with the iron-copper-carbon system, the dimensional change at different combined carbon content and different sintered densities was evaluated. The performance of Astaloy CrL warm compacted is also included. The result are presented in figure 6 for compaction at 43.5tsi followed by sintering at 2050°F for 30 minutes in 90/10 N_2/H_2.

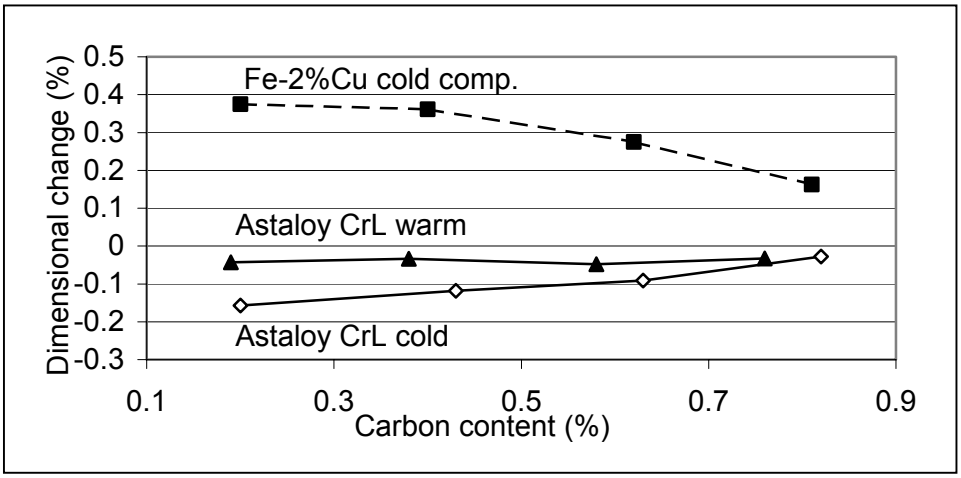


Figure 6. Dimensional change for Astaloy CrL (material A) and Fe-2%Cu (material B) at different combined carbon content.

Material B shows swelling in the carbon range from 0.2 to 0.8%. Material B is sensitive for carbon content above 0.4% regarding dimensional change. Small change of combined carbon content cause a significant more scatter in dimensional change.

Evaluation of the dimensional change at different sintered density levels is presented for material B in figure 7a, for material A cold compacted in figure 7b and warm compacted in figure 7c.

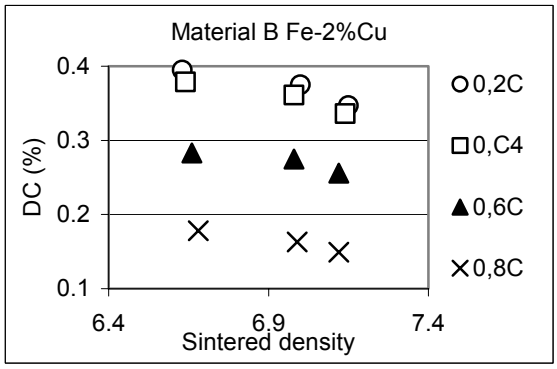


Figure 7a DC vs. SD, material B cold comp.

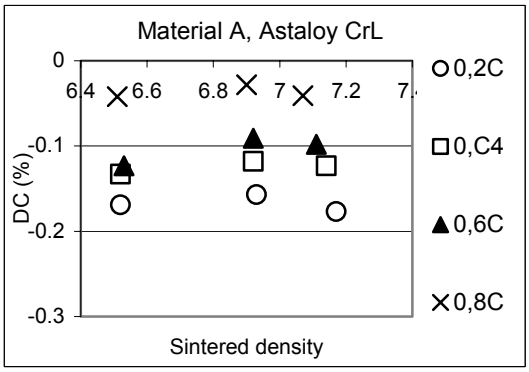


Figure 7b. DC vs. SD, material A cold comp.

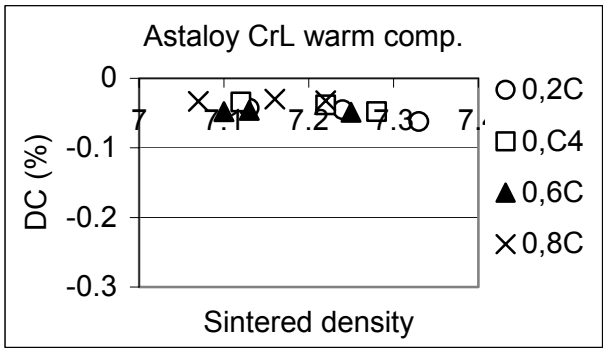


Figure 7c. DC vs. SD, material A. warm compacted.

Material A shows a more stable dimensional change if compared to material B both for variation in density as well as carbon content. Dimensional change varies between 0.05 and 0.2% for material A and 0.15 to 0.4% for material B in the density range of 6.5 to 7.2 g/cm^3 and carbon rage of 0.2 to 0.8%. Adopting warm compaction the dimensional change for material A is closer to zero figure 7c and nearly independent of sintered density. Level of combined carbon seems to have very little effect on the dimensional change.

Sinterhardening.

Chromium as an alloying element in steel gives a high hardenability. CCT diagram for material A at a carbon content 0.6% and a sintered density of 7.0 g/cm^3 reported in figure 8a shows the potential of the material. Figure 8b shows the phase amount of the same composition plotted vs cooling rate.

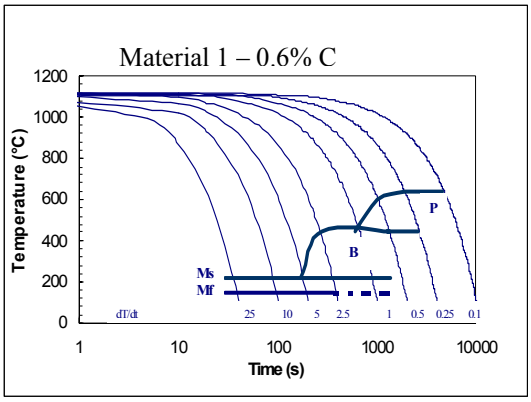


Figure 8a. CCT diagram material A + 0.6% C

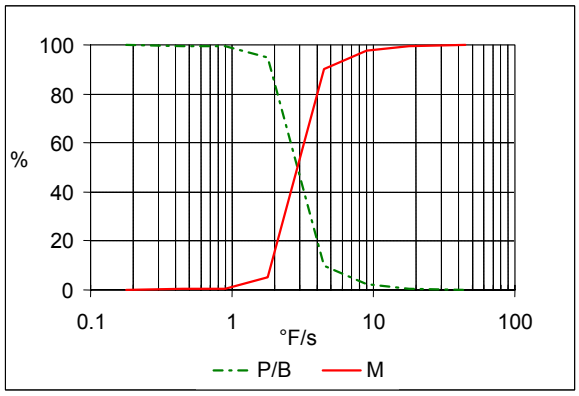


Figure 8b Phase amount mtrl 1 + 0.6%C.

Material A at a carbon content of 0.6% has a transformation to 100% martensite at a cooling rates above 11°F/s. Analyses of phase amount states that a cooling rate of 3°F/s is needed to obtain more than 50% martensite. This shows the possibilities to use the material for sinterhardening applications.

For sinterhardening grades addition of copper is often used in order to increase the hardenability. Addition of Nickel in order to improve hardenability is also possible. Admixture of copper or nickel decreases the need of either density or cooling rate to obtain a microstructure of more than 50% martensite or hardness above 30 HRC.

To verify the possibility to use Astaloy CrL in sinterhardening application an investigation with different amount of copper, 1 and 2% is performed. Astaloy CrL is compared to D.DH-1, diffusion bonded 2% Cu to pre-alloyed 1.5% molybdenum base powder. In table 8 the mechanical properties obtained at a compacting pressure of 43.5tsi (600Mpa) sintered at 2050°F (1120°C) with a cooling rate of 4.5°F/s (2.5°C/s) is shown. Tempering is done at 356°F (200°C) for 60 minutes.

Table 8. Mechanical Properties, Sinterhardening

	UTS ksi(Mpa)	YS ksi(MP)	HRC	A %
Mtrl A + 2% Cu – 0.6% C	129.7 (894)	123.9 (854)	31	0.27
Mtrl A + 2% Cu – 0.8% C	114.7 (791)	107.8 (743)	34	0.21
Mtrl A + 1% Cu – 0.6% C	129.4 (892)	113.0 (779)	29	0.37
Mtrl A + 1% Cu – 0.8% C	107.0 (738)	-*	35	0.19
Mtrl D + 0.6% C	123.0 (848)	105.0 (724)	25	0.53
Mtrl D+ 0.8% C	113.1 (780)	104.3 (719)	36	0.29

- No value, elongation below 0.2%

From the evaluation it can bee seen that the hardness increases with carbon content while UTS and YS decreases. The decrease is caused by increased amount of martensite and retained austenite in the microstructure. UTS and YS has an optimum for material A at a carbon content of 0.6% for both 1 and 2% added copper. Material D has a lower hardenability if compared to material A with copper additions.

Fatigue performance

Material A is evaluated regarding bending fatigue after sintering at 2050°F (1120°C) for 30 minutes in 90/10 N_2/H_2 atmosphere with a cooling rate of 1.4°F/s (0.8°C/s) at a sintered density of 7.1 g/cm3. Evaluation of the fatigue performance at 0.55 and 0.74% C is presented.

Evaluation of S-N curve is done in four point bending mode at a load ratio of R = -1 and a frequency of 25 Hz. Testing is interrupted when compliance increases in order to stop the test before final rupture occurs [4]. The reason for this is to be able to detect the crack initiation and crack propagation at an early stage. S-N curve for material A at a carbon content of 0.55% is shown in figure 9.

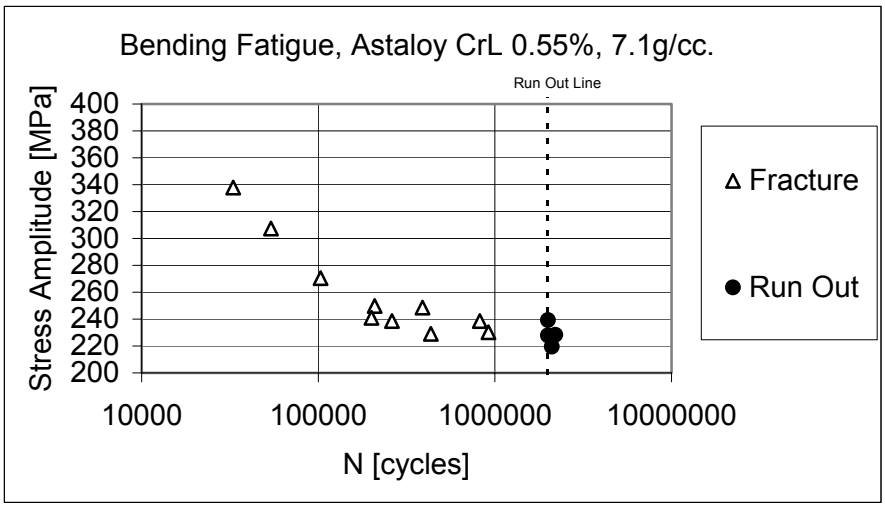


Figure 9. S-N curve material A+0.55% C.

An endurance limit of 236 MPa with a standard deviation of 6 MPa is found for the material.

From the fractography investigation the crack nucleation occur in an area of low density. This acts as a stress concentrator, see square in figure 10 a. No surface pore was found in this area in this

specimen. The early crack propagation is trans-particle, see figure 12. The final propagation is dominated by fine ductile rupture with a few cleavage facets, figure 11.
The fatigue fracture of the material appears overall ductile. This is based on the fact that no inter-granular propagation is observed in the initiation area.

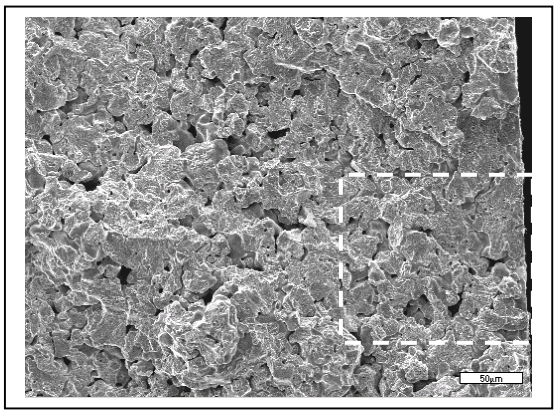


Figure 10a. Nucleation site. 330X.

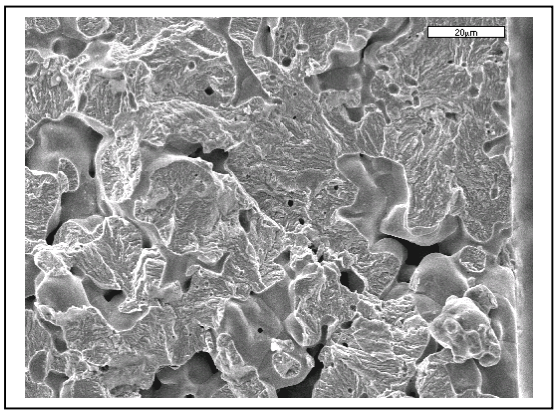


Figure 10b. Nucleation site. 1000X

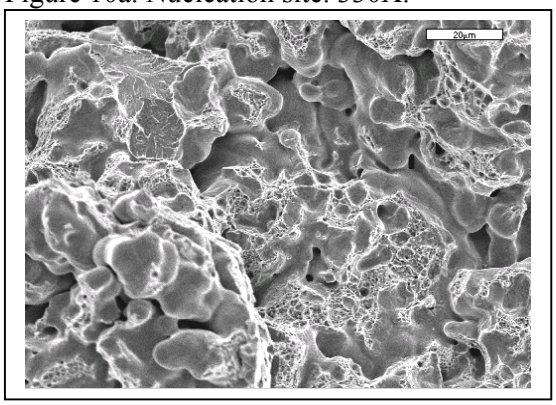


Figure 11. Fast crack propagation area.

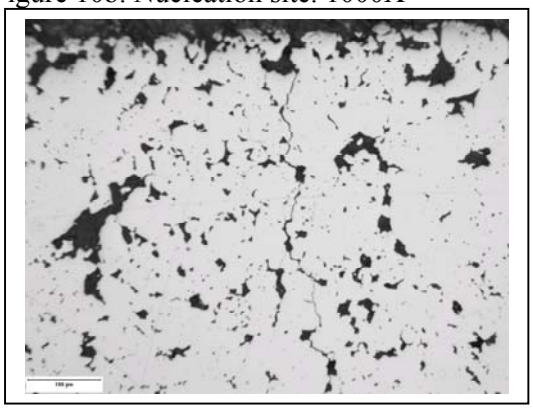


Figure 12 Unetched. crack propagation

S-N curve for material A at a carbon content of 0.74 is shown in figure 13.

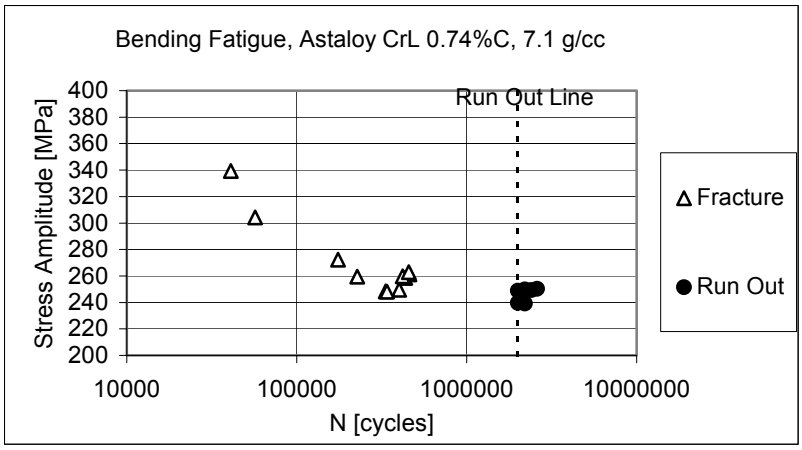


Figure 13. S-N curve material A+0.74% C

This shows an endurance limit of 252 MPa with a standard deviation of 3 MPa

The fractography investigation of several bars shows that the crack nucleation occurred at the edge of the cross section, due to an area with lower density or by a pore facing the surface figure 14a and b. The fracture is fully trans-particles and trans-granular in the initiation site, figure 14.
Observation in the final propagation area, figure 15 confirms the absence of fast fracture features: no cleavage and no inter-granular fracture are observed. Fracture surface is in this area characterized by dimples, mainly through the sinter necks walk i.e. inter-particle but trans-granular fracture.
All these indexes confirm the ductile fatigue fracture behavior of this material
Fast propagation features fully consist of dimples.

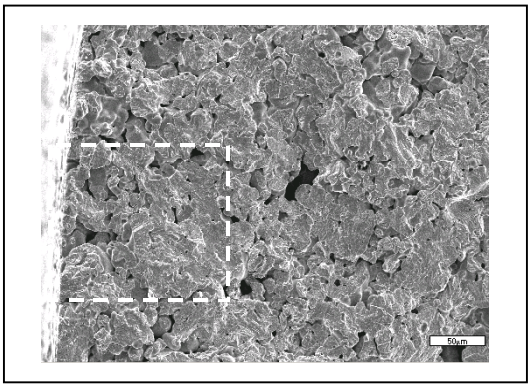


Figure 14a Nucleation site.

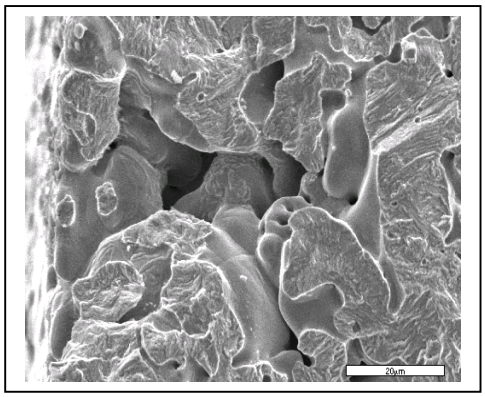


Figure 14b Nucleation site.

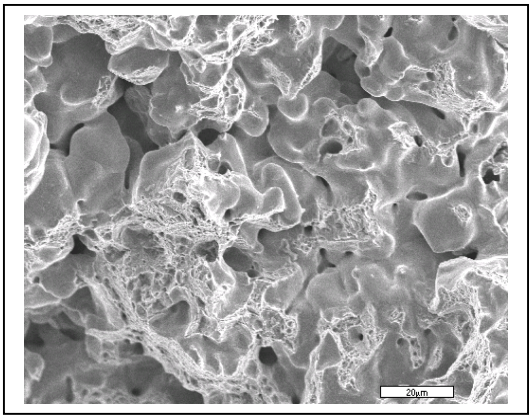


Fig 15. Fast crack propagation area.

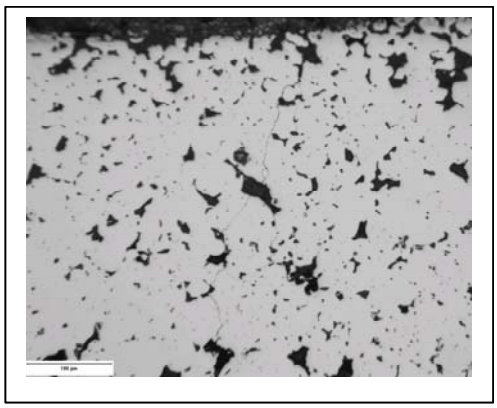


Figure 14 Crack propagation

Sintering atmosphere

Control of sintering atmosphere is important for chromium containing materials. From the Richardsson- Ellingham diagram oxidation of chromium (2050°F) starts at ~$1*10^{19}$atm oxygen. In this case the activity of chromium is 1. In pre-alloyed state the activity at low amount of chromium could approximately be set equal to the weight percent of chromium. In figure 16a decarburization and oxidation for material A + 0.2% C at different partial pressure of oxygen is presented. In figure 16b the behaviour for material A+ 0.6% C at different partial pressure of oxygen is shown. Analysed carbon and oxygen are as mean values for the cross section of the specimens. The experiment is performed in a laboratory belt furnace at 2050°F for 30 minutes at temperature. The lowest partial pressure of oxygen is reached by use of dissociated ammonia. The other points are achieved in 90/10 N_2/H_2. In order to achieve a logpO_2 of –16 and of –14, the sintering atmosphere 90/10 N_2/H_2 was bubbled though water. No hydrocarbon is added to the sintering atmosphere.

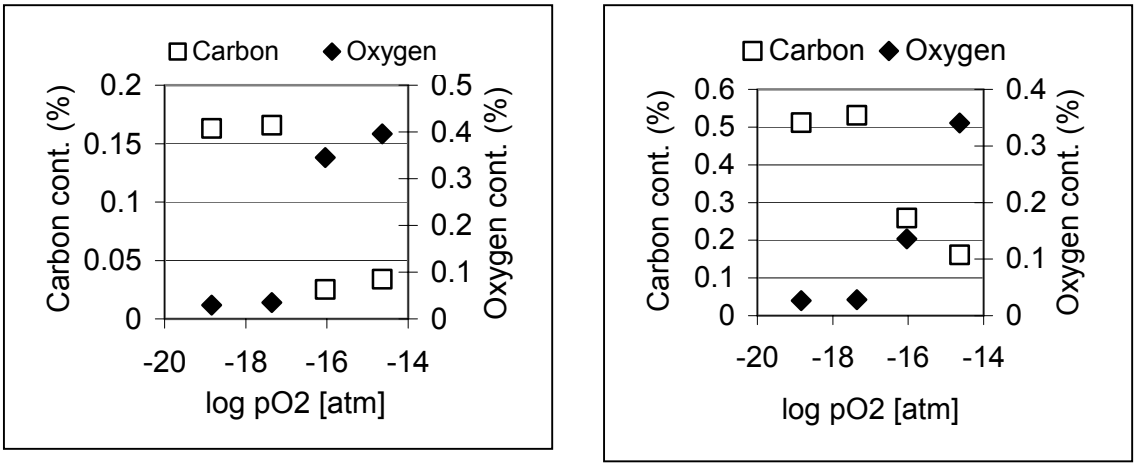


Figure 16 a and b. Decarburisation and oxidation of a) material A + 0.2 and b) material A + 0.6% C at different partial pressures of oxygen.

At a partial pressure of $4*10^{-18}$ atm (log pO_2 = -17.36) there is hardly any decarburisation excluded the one that appears due to reduction of chromium oxides. At $9*10^{-17}$ atm (log pO_2 = -16.04) the oxygen in the atmosphere reacts with carbon in the parts causing decarburization and with chromium causing formation of chromiumoxides this both at 0.2 and 0.6% C.

CONCLUSIONS

1. Astaloy CrL a prealloyed material with 1.5% Cr and 0.2% Mo cold compacted and sintered at 2050°F has mechanical properties equal or better than D.AB and excide the FC0200 system.

2. At a sintering temperature of 2050°F and a cooling rate of 1.4°F/s the material undergoes a transformation from ferrite/perlite to bainite in the microstructure in the carbon range from 0.2 to 0.8%. This results in increased UTS from 50 to 110 ksi, increased yield strength from 20 to 100 ksi and increased hardness from 100 to 250 Vickers

3. Warm compaction increases the density by 0.15 to 0.2 g/cm^3. This can be compared to an increase in compaction pressure of 14.5tsi if cold compaction is adopted. UTS and YS improves by 10 to 20%. Elongation increases with 50 to 100%

4. High temperature sintering is beneficial for chromium containing material. UTS of 132.4ksi at 0.51% C and 157 ksi at 0.66% C is obtained..

5. Astaloy CrL is more dimensional stable than FC-0200/0208

6. Astaloy CrL with copper addition can be used for sinterhardening applications
HRC > 30 is obtained at a cooling rate of 4.5°F/s

7. Endurance limit for Astaloy CrL + 0.55%C at a sintered density of 7.1g/cm^3 and sintering at 2050°F is 236 MPa with a stdav. of 6MPa.
Endurance limit for Astaloy CrL + 0.74%C and same processing conditions is 252Mpa stdav of 3Mpa.

8. Addition of hydrocarbon to the sintering atmosphere or graphite addition in order to correct the decarburisation which occur throughout the material due to reduction of chromium oxides is recommended.

REFERENCE

1. Engström. U; Johansson B.; ”Experience with Warm Compaction of Densmix Powders in the Production of Complex Parts”: Powder Metallurgy World Congress. Kyoto Japan November 2000

2. Engström. U; Johansson B.. Rassmuss J.; ”High Performance Material of Warm Compacted High Strength Sintered Steels”: Powder Metallurgy World Congress. Granada. Spain. October. 1998.

3. U. Engström. “ Evaluation of sintering hardening of different PM materials”. PM^2TEC 2000. New York . 2000

4. Bergmark A.. Alzat L.. Persson U. “ Fatigue Crack Initiation in PM Steel”. To bee presented at PM^2TEC 2000. Orlando 2002